


Sulfur availability for *Vibrio fischeri* growth during symbiosis establishment depends on biogeography within the squid light organ

Nathan P. Wasilko, Jessie Larios-Valencia[†],
Caroline H. Steingard[‡], Briana M. Nunez,
Subhash C. Verma[§] and Tim Miyashiro⁺ 

Department of Biochemistry and Molecular
Biology, Pennsylvania State University, 410 South Frear
Laboratory, University Park, PA 16802, USA.

Summary

The fitness of host-associated microbes depends on their ability to access nutrients *in vivo*. Identifying these mechanisms is significant for understanding how microbes have evolved to fill specific ecological niches within a host. *Vibrio fischeri* is a bioluminescent bacterium that colonizes and proliferates within the light organ of the Hawaiian bobtail squid, which provides an opportunity to study how bacteria grow *in vivo*. Here, the transcription factor CysB is shown to be necessary for *V. fischeri* both to grow on several sulfur sources *in vitro* and to establish symbiosis with juvenile squid. CysB is also found to regulate several genes involved in sulfate assimilation and to contribute to the growth of *V. fischeri* on cystine, which is the oxidized form of cysteine. A mutant that grows on cystine but not sulfate could establish symbiosis, suggesting that *V. fischeri* acquires nutrients related to this compound within the host. Finally, CysB-regulated genes are shown to be differentially expressed among the *V. fischeri* populations occupying the various colonization sites found within the light organ. Together, these results suggest the biogeography of *V. fischeri* populations within the squid light organ impacts the physiology

of this symbiotic bacterium *in vivo* through CysB-dependent gene regulation.

Introduction

Plants and animals house microbiomes that impact their physiology, development and evolution (Gilbert *et al.*, 2015). The disruption of a microbiome either through chemical or physical perturbation typically has a negative consequence on the overall fitness of the host (Reid *et al.*, 2011). Despite the increased awareness of the important roles these microbiomes play in regulating states of health and disease, the factors that contribute to the fitness of most microbial species *in vivo* remain poorly understood. Understanding the factors that impact the fitness of host-associated microbes ultimately depends on determining the mechanisms they use to acquire nutrients and energy for growth *in vivo*. For microbes that associate with their host in an extracellular manner, the variability in environmental conditions among potential colonization sites within the host represents a challenge for studying those mechanisms (Meadows and Wargo, 2014). However, approaches that account for the spatial organization of host-associated microbial populations, i.e. their biogeography, have the potential to reveal mechanisms that impact microbial fitness at specific colonization sites (Stacy *et al.*, 2016).

An experimental system that is particularly amenable to biogeographical studies is the symbiosis established between *Euprymna scolopes* (Hawaiian bobtail squid) and the marine bacterium *Vibrio fischeri* (McFall-Ngai, 2014). Shortly after juvenile squid hatch from their eggs, they acquire *V. fischeri* cells from the seawater environment, which quickly colonize three epithelium-lined crypt spaces located on either side of the host's light organ. *V. fischeri* is a genetically tractable microbe, and the juvenile light organ is amenable to light microscopy, which has led to the use of fluorescent proteins as markers of cell position and gene expression *in vivo* (Dunn *et al.*, 2006; Sun *et al.*, 2015). The populations resulting from the rapid proliferation of the founder cells that initially colonize the

Accepted 27 November, 2018. *For correspondence. E-mail tim14@psu.edu; Tel. (814) 865-1916; Fax (814) 863-7024. Present addresses: [†]Medical Scientist Training Program, Albert Einstein College of Medicine, Bronx, NY 10461, USA; [‡]Department of Microbiology, Cornell University, Ithaca, NY 14853, USA; [§]Laboratory of Molecular Biology, Center for Cancer Research, National Cancer Institute, National Institutes of Health, Bethesda, MD 20892, USA.

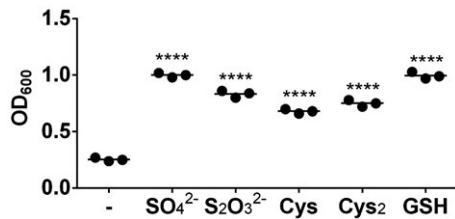


Fig. 1. Impact of sulfur source on growth of *V. fischeri*. *V. fischeri* strain ES114 was grown for 21 h in sulfur-free medium supplemented with the indicated sulfur source (– = no supplement, SO₄²⁻ = 1 mM sulfate, S₂O₃²⁻ = 0.5 mM thiosulfate, Cys = 1 mM cysteine, Cys₂ = 0.5 mM cystine and GSH = 1 mM glutathione). Reported OD₆₀₀ values were calculated using a sample containing only media as a blank. Each point represents an independent biological replicate, and the bar represents the mean ($n = 3$). One-way ANOVA revealed significant differences among means ($F_{5,12} = 361.7$, $p < 0.0001$). A Dunnett's *post-hoc* test was performed to statistically compare the means of each group containing a sulfur source to the mean of the no-supplement group, with p -values adjusted for multiple comparisons (**** = $p < 0.0001$). Experiment was performed three times with similar results obtained among each trial.

crypt spaces produce bioluminescence that the host uses as a form of camouflage (Jones and Nishiguchi, 2004). Bacterial bioluminescence is a product of the enzyme luciferase, which releases light while consuming reducing power and oxygen (Meighen, 1993). Oxygen is transported from the gills to the bacterial populations via the carrier protein hemocyanin (Kremer *et al.*, 2014). The affinity of hemocyanin for oxygen is positively correlated with pH (Kremer *et al.*, 2014), and, within the crypt spaces of adult animals, *V. fischeri* promotes the release of oxygen by acidifying the environment through the fermentation of host-derived chitin (Schwartzman *et al.*, 2015).

While chitin fermentation appears to fuel the growth of *V. fischeri* in the mature symbiosis, the mechanisms that support bacterial growth within the juvenile light organ are less clear. The expression of genes necessary for metabolizing chitin byproducts are repressed by NagC (Sun *et al.*, 2015), suggesting that nutrients other than chitin are accessed by the corresponding *V. fischeri* populations at this early stage of symbiosis. The current model is that host proteins are degraded into peptides and amino acids that promote *V. fischeri* growth, which was initially proposed from the successful colonization of juvenile animals by mutants that exhibit auxotrophy for various amino acids (Graf and Ruby, 1998). One amino acid considered in this study was cysteine, which is particularly interesting because its biosynthesis also represents the primary mechanism for a bacterium to convert an inorganic sulfur source, e.g. sulfate, into an organic form that fuels growth. The cysteine auxotroph was supported to 5% of wild-type bacterial levels *in vivo* (Graf and Ruby, 1998), raising the possibility that *V. fischeri* can utilize an organic form of sulfur for growth within the light organ. The mutation within

the cysteine auxotroph used in this study remains undefined; however, more recently, a Δ *cysK* mutant, which fails to grow on sulfate due to its inability to synthesize cysteine from the precursors *O*-acetyl-serine and sulfide, was shown to achieve normal bacterial levels *in vivo* (Singh *et al.*, 2015), which is consistent with *V. fischeri* having access to an organic sulfur source within the juvenile light organ that promotes growth *in vivo*.

In this study, the ability of *V. fischeri* to grow on various sulfur sources *in vitro* is used to gain insight into the sulfur sources that facilitate growth of *V. fischeri* within the squid light organ. The transcription factor CysB is shown to regulate genes necessary for growth on several sulfur sources. Squid colonization assays with defined mutants involving CysB revealed that the ability of *V. fischeri* to grow on cystine, which is the oxidized form of cysteine, is a trait that is important for symbiosis establishment. Finally, the expression of CysB-regulated genes is shown to differ among the *V. fischeri* populations that occupy different crypt spaces within the juvenile light organ, suggesting the bioavailability of host-derived sulfur sources varies according to the biogeography of the bacteria *in vivo*. Together, these findings increase understanding of the molecular mechanisms that promote microbial fitness within host environments.

Results

CysB promotes growth of *V. fischeri* on various sulfur sources

V. fischeri grows in defined minimal medium containing sulfate as the sole sulfur source (Sun *et al.*, 2015), which shows that *V. fischeri* has the ability to assimilate sulfate. To determine whether *V. fischeri* grows on other sulfur sources, we measured the growth yield of the wild-type, symbiotic *V. fischeri* strain ES114 (Ruby *et al.*, 2005) in sulfur-free medium supplemented with sulfate, thiosulfate, cysteine, cystine or glutathione, which are sulfur sources commonly used by other γ -proteobacteria (Kredich, 1996). The concentration of each supplemented compound was set so that the concentration of sulfur atoms in each experimental group was 1 mM. After 21 h, some background growth occurred in sulfur-free medium (Fig. 1), suggesting a contaminating sulfur source is present in the base medium, which is similarly observed in studies of sulfate assimilation by other bacteria (Chonoles Imlay *et al.*, 2015). However, supplementation with 1 mM sulfate resulted in a growth yield 3.9-fold higher (Fig. 1), demonstrating that the unknown sulfur source is growth-limiting within the sulfur-free medium and that the assay is sufficient for identifying sulfur-containing compounds that promote bacterial growth. Other compounds that promote the growth of *V. fischeri* include

thiosulfate, cysteine, cystine and glutathione (Fig. 1), on which other γ -proteobacteria like *Escherichia coli* and *Salmonella typhimurium* can grow (Kredich, 1996).

In γ -proteobacteria, sulfate assimilation depends on several genes (referred to as *cys* genes) involved in transporting sulfate into the cell and reducing it to sulfide, which can then be used for anabolic purposes, including cysteine biosynthesis (Kredich, 1996). The transcription of *cys* genes is regulated by the LysR-type transcription factor CysB (Kredich, 1992). Within the genome of ES114, the gene annotated as the *cysB* homologue is *VF_1490* (Fig. 2A). *VF_1490* is predicted to encode a 36.1 kDa protein with 324 amino acids and 74% identity to the CysB protein of *E. coli*. We replaced *VF_1490* in ES114 by allelic exchange with a deletion allele (Δ *cysB*), which lacks the codons for residues 26–323 (Fig. 2A). Unlike wild-type cells, Δ *cysB* failed to grow on sulfate, but the mutant could grow on cysteine (Fig. 2B), indicating that it is a cysteine auxotroph, as observed with *cysB*⁻ mutants of other γ -proteobacteria (Kredich, 1996). The mutant failed to grow on thiosulfate and cystine (Fig. 2B), suggesting that *VF_1490* regulates genes that permit growth on these sulfur sources. The

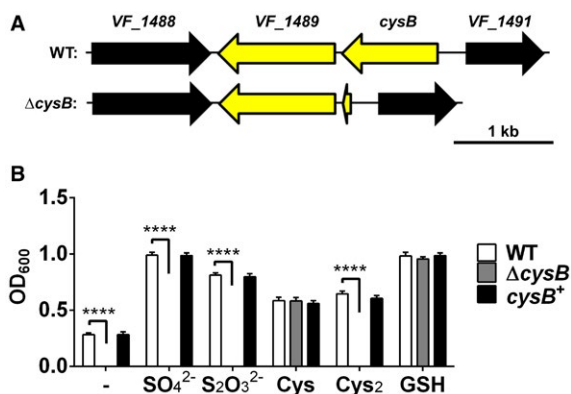


Fig. 2. Impact of CysB on growth of *V. fischeri* on various sulfur sources.

A. Above, genetic locus of *VF_1490* (yellow arrow labeled *cysB*) in the genome of wild-type strain ES114. *VF_1489* is predicted to encode a SAM-dependent methyltransferase. Below, corresponding region in the in-frame *cysB* deletion mutant (Δ *cysB*) constructed in this study.

B. *V. fischeri* strains (WT = TIM313, Δ *cysB* = TIM410 and *cysB*⁺ = TIM409) were grown for 21 h in sulfur-free medium supplemented with the indicated sulfur source (– = no supplement, SO₄²⁻ = 1 mM sulfate, S₂O₃²⁻ = 0.5 mM thiosulfate, Cys = 1 mM cysteine, Cys₂ = 0.5 mM cystine and GSH = 1 mM glutathione). Reported OD₆₀₀ values were calculated using a media-only sample as a blank. Graphical and error bars represent means and standard deviations of independent biological replicates ($n = 3$) respectively. Two-way ANOVA revealed significant differences among means due to sulfur source ($F_{5,36} = 1193$, $p < 0.0001$), genotype ($F_{2,36} = 2403$, $p < 0.0001$), and their interaction ($F_{10,36} = 336.6$, $p < 0.0001$). A Dunnett's *post-hoc* test was performed to statistically compare the means of each mutant to wild type for each sulfur treatment, with p -values adjusted for multiple comparisons (**** = $p < 0.0001$; comparisons with $p \geq 0.05$ are considered not significant and are not labeled). Experiment was performed three times with similar results obtained among each trial.

Δ *cysB* mutant grew on glutathione (Fig. 2B), indicating that growth of *V. fischeri* on this compound is independent of *VF_1490*. We also tested for genetic complementation by introducing the *VF_1490* gene with its native promoter in single copy into the genome of the Δ *cysB* mutant and found using the panel of sulfur-containing compounds that this strain (*cysB*⁺) grew similarly to wild-type cells (Fig. 2B). Together, these results suggest that *VF_1490* encodes the CysB homologue of *V. fischeri* that plays a role in promoting growth on various sulfur sources.

CysB promotes the establishment of symbiosis with *E. scolopes*

To determine whether CysB impacts how *V. fischeri* establishes symbiosis with *E. scolopes*, we conducted squid colonization assays (Fig. 3A). These assays require a *V. fischeri* inoculum in filter-sterilized seawater (FSSW), which contains 27.7 mM sulfate. Because the Δ *cysB* mutant fails to grow in medium containing sulfate as the sole sulfur source (Fig. 2B), we were concerned that the mutant would exhibit reduced fitness in FSSW, which could complicate interpreting the results from the colonization assay. Therefore, in assays involving the Δ *cysB* mutant, the initial inoculum of the mutant was elevated up to 10-fold above wild type, which was a level sufficient for the abundance of Δ *cysB* to stay at or above that of wild type in FSSW for 3.5 h (Fig. 3B).

At 48 h post-inoculation (p.i.), all animals exposed to wild-type cells exhibited luminescence (Fig. 3C) and contained CFU (Fig. 3D), consistent with ES114 having colonized each animal's light organ. In contrast, the majority of animals exposed to the Δ *cysB* mutant did not exhibit luminescence (Fig. 3C). However, all of these animals contained CFU but at levels approximately 250-fold lower than that of animals containing WT cells (Fig. 3D). One possible reason for decreased abundance of the Δ *cysB* mutant *in vivo* is if this mutation impairs the ability of *V. fischeri* to produce luminescence, which is necessary for the populations of *V. fischeri* that have resulted from the successful colonization of the squid host to be subsequently maintained (Visick *et al.*, 2000; Verma and Miyashiro, 2013; Studer *et al.*, 2014). However, when grown in the presence of *N*-3-oxohexanoyl homoserine lactone (3-oxo-C6 HSL), which is a small signaling molecule associated with quorum sensing that stimulates bioluminescence production by *V. fischeri* (Miyashiro and Ruby, 2012), cultures of the Δ *cysB* mutant produced bioluminescence (Fig. S1). Thus, these results suggest that the low levels of luminescence associated with animals colonized by the Δ *cysB* mutant (Fig. 3C) is more likely due to the corresponding populations being too small for quorum sensing to promote detectable bioluminescence. We also found that mutants containing transposon insertions in *cysK*, *cysJ* or *cysD* are

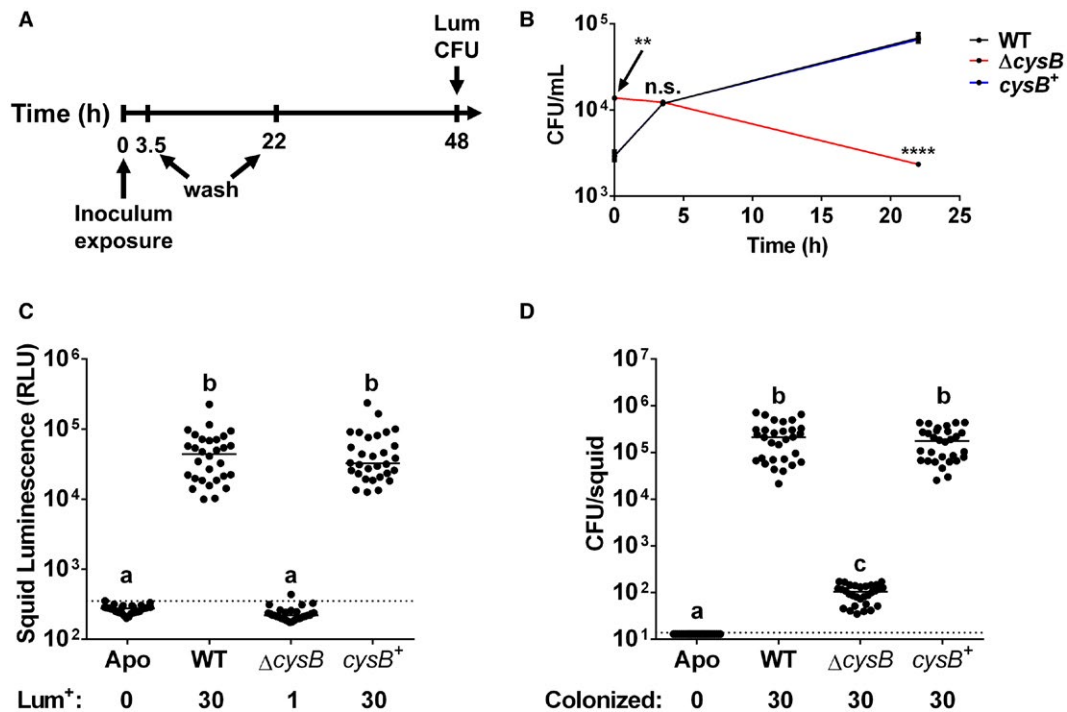


Fig. 3. Impact of CysB on the ability of *V. fischeri* strains to establish a symbiotic association with *E. scolopes* juveniles. Strains used in these experiments are TIM313 (WT), TIM410 ($\Delta cysB$) and TIM409 (*cysB*⁺).

A. Timeline of squid colonization assay. Each wash step involves the transfer of the animal to fresh FSSW.

B. Abundance of *V. fischeri* strains in FSSW over time. Points and error bars represent the means and standard deviations of independent biological replicates ($n = 3$) respectively. Two-way ANOVA revealed significant differences among means due to genotype ($F_{2,18} = 68.96$, $p < 0.0001$), time ($F_{2,18} = 289.2$, $p < 0.0001$) and their interaction ($F_{4,18} = 121.2$, $p < 0.0001$). A Dunnett's *post-hoc* test was performed to statistically compare the means of each mutant to wild type for each time point, with p -values adjusted for multiple comparisons (**** = $p < 0.0001$, ** = $p < 0.01$, n.s. = $p \geq 0.05$). Experiment was performed three times with similar results obtained among each trial.

C. Luminescence of animals exposed to indicated *V. fischeri* strains. Apo = apo-symbiotic. Each point represents the luminescence of each animal ($n = 30$ /group) at 48 h p.i. The dotted line indicates the cutoff above which animals are scored as luminescent (Lum⁺) and was calculated by performing a one-tailed *t*-test of Apo group ($\alpha = 0.01$). Lum⁺ animal counts are shown below the name of each group. A Kruskal–Wallis test revealed significant differences among group medians ($H = 92.93$, d.f. = 3, $p < 0.0001$). A Dunn's *post-hoc* test was performed to statistically compare the medians of each group, with p -values adjusted for multiple comparisons. Comparisons between groups with different letters have significantly different medians ($p < 0.0001$), and comparisons between groups with the same letter do not have significantly different medians ($p \geq 0.05$).

D. CFU levels of animals in C. Each point represents the CFU level of one animal. Dotted line indicates the limit of detection (14 CFU/squid). A Kruskal–Wallis test revealed significant differences among group medians ($H = 102.1$, d.f. = 3, $p < 0.0001$). A Dunn's *post-hoc* test was performed to statistically compare the medians of each group, with p -values adjusted for multiple comparisons. Comparisons between groups with different letters have significantly different medians (a/b and $b/c = p < 0.0001$, $a/c = p < 0.01$), and comparisons between groups with the same letter do not have significantly different medians ($p \geq 0.05$). Experiment was performed twice with similar results obtained among both trials.

cysteine auxotrophs (Fig. S2) and can establish symbiosis (Fig. S3A and B), suggesting that the growth defect of the $\Delta cysB$ mutant *in vivo* is independent of its failure to grow on sulfate. Finally, animals exposed to the *cysB*⁺ mutant displayed levels of luminescence and CFU comparable to animals colonized by WT (Fig. 3C and D), demonstrating genetic complementation with *cysB*. Together, these results suggest that CysB is necessary for *V. fischeri* cells to grow to wild-type levels within the environment of the light organ.

Regulation of *cys* genes in *V. fischeri*

Our results above suggest that CysB promotes the growth of *V. fischeri* within the squid light organ. To gain

insight into how CysB contributes to symbiosis establishment, we investigated the function of CysB as a transcriptional regulator in *V. fischeri*. During sulfate assimilation by other γ -proteobacteria, CysB promotes the expression of *cys* genes to facilitate the transport of sulfate into the cytoplasm and its reduction to sulfide (Kredich, 1992), which can then be used for cysteine biosynthesis (Fig. 4A). Cytoplasmic cysteine indirectly impacts this regulatory function of CysB: cysteine inhibits the enzymatic activity of CysE, which catalyzes the synthesis of the CysB inducer, *N*-acetyl-serine (NAS) (Kredich and Tomkins, 1966). Thus, at high cysteine levels, NAS levels decrease, which leads to lower transcription of the *cys* genes. Therefore, the expression level of a *cys* gene

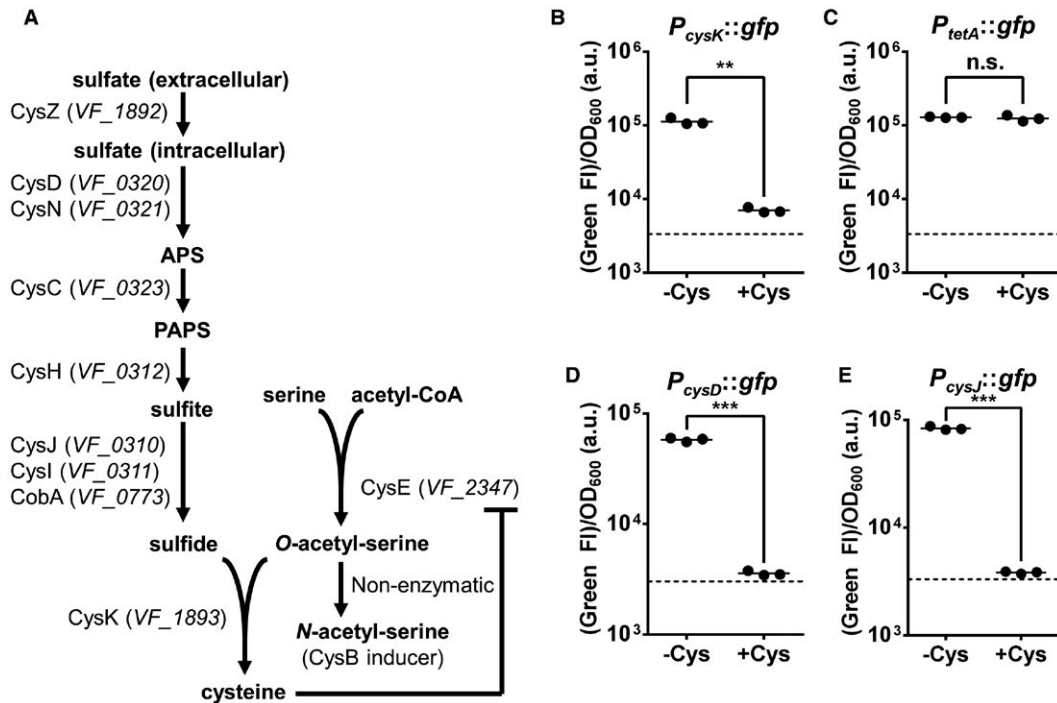


Fig. 4. Impact of cysteine on expression of *cys* genes in *V. fischeri*.

A. Model of sulfate assimilation and cysteine biosynthesis for *V. fischeri* ES114. Genes predicted to facilitate enzymatic steps are located next to each arrow. APS = adenosine-5' phosphosulfate, PAPS = 3'-phosphoadenosine-5'-phosphosulfate. Feedback inhibition of CysE by cysteine is also shown.

B–E. Wild-type ES114 harboring a reporter plasmid for the indicated promoter was grown in sulfate-replete minimal medium \pm 1 mM cysteine. Plasmids used are pVF_1893P (**B**), pSCV26 (**C**), pVF_0320P (**D**) and pVF_0310P (**E**). Gene expression was determined by normalizing the green fluorescence of an individual culture sample with its corresponding OD₆₀₀ (a.u. = arbitrary units). Each point represents an independent biological replicate, and the bar represents the mean ($n = 3$). The dotted line indicates the background level of normalized fluorescence for a non-fluorescent control (pVSV105/ES114). For each experiment, an unpaired, two-tailed *t* test with Welch's correction was performed to determine statistical differences between group means (n.s. = not significant, ** = $p < 0.01$, *** = $p < 0.001$). Each experiment was performed three times with similar results obtained among trials for each promoter.

within a *V. fischeri* population provides a readout for the regulatory activity of CysB within those cells.

To study *cys* gene expression, we constructed reporter plasmids for three promoter regions: *cysK* (P_{cysK}), *cysDN-yfbS-cysD* (P_{cysD}) and *cysJIH* (P_{cysJ}). For each construct, a promoter region was cloned upstream of *gfp* in the plasmid pTM267 (Miyashiro *et al.*, 2010), which we have previously used for examining gene expression of *V. fischeri* (Sun *et al.*, 2015). For cultures of cells harboring a reporter plasmid, the GFP/OD₆₀₀ ratio can be used as a quantitative measure of the transcriptional expression by the corresponding promoter. We first tested the response of these reporter constructs using 1 mM cysteine, which results in decreased expression of *cys* genes in other γ -proteobacteria (Kredich and Tomkins, 1966). In response to 1 mM cysteine, expression of P_{cysK} in wild-type cells decreased 29.6-fold (Fig. 4B), which suggests the regulatory network controlling *cysK* transcription in *V. fischeri* functions similarly to those of other γ -proteobacteria. As a negative control for *cys* genes, we also used cells containing a reporter for the *tetA* promoter (P_{tetA}),

which is expressed in the absence of the TetR repressor (Hillen and Berens, 1994). Cells harboring the P_{tetA} reporter plasmid showed no change in expression in response to 1 mM cysteine (Fig. 4C), suggesting that the decreased expression of P_{cysK} in response to exogenous cysteine (Fig. 4B) is specific to this promoter and not due to cysteine affecting the fluorescence properties of GFP. In response to exogenous cysteine, expression of P_{cysD} and P_{cysJ} decreased 101- and 157-fold respectively (Fig. 4D and E), which is similar to the effect observed with *cysK*. Together, these results show that the presence of exogenous cysteine results in repression of *cys* genes in *V. fischeri*, which is consistent with their transcription being indirectly controlled by feedback inhibition (Fig. 4A).

We next sought to determine the dependency of *cys* gene expression on CysB in *V. fischeri*. However, because the $\Delta cysB$ mutant is a cysteine auxotroph (Fig. 2B), it was not possible to grow this mutant using sulfate as the sole sulfur source for measuring *cys* gene expression under the inducing conditions associated with sulfate assimilation. Therefore, as an alternative approach, we asked whether

amino acid substitutions within CysB could be made to induce the expression of *cys* genes in cells grown under cysteine-replete conditions, which permit the growth of cysteine auxotrophs (Fig. 2B). Residues 86–324 within the CysB homologue of *S. typhimurium* forms a structure that binds NAS (Mittal *et al.*, 2017), which alters the activity of CysB as a transcription factor via allostery. In *E. coli*, certain amino acid substitutions within the inducer region impact the ability of CysB to regulate transcription of *cys* genes (Lochowska *et al.*, 2001). In particular, substitution of Ala-227 with Asp results in a CysB variant (CysBA227D) that shows strong binding to and transcriptional activation of CysB-induced promoters independent of NAS (Lochowska *et al.*, 2001). The Ala-227 residue is conserved in the CysB homologue of *V. fischeri* (Fig. S4), which enabled construction of a *cysBA227D* allele by site-directed mutagenesis. This allele was introduced into the genome of the $\Delta cysB$ mutant *in trans*, resulting in the mutant *cysBA227D*. In the presence of 1 mM cysteine, expression of *cysK* was 3.0 ± 0.2 times higher in the *cysBA227D* mutant than in wild-type cells (Fig. 5), suggesting that the CysBA227D variant induces expression of *cys* genes under cysteine-replete conditions. This result is consistent with *V. fischeri* using CysB to regulate expression of *cys* genes in response to cysteine.

CysBA227D promotes growth of *V. fischeri* on cystine

Our results with the *cysBA227D* mutant suggest that CysBA227D promotes some expression of *cys* genes. To

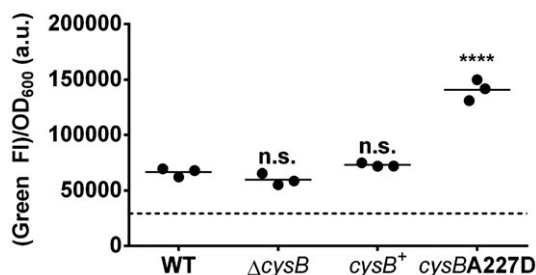


Fig. 5. Impact of CysB on expression of *cys* genes in *V. fischeri*. Indicated strains harboring the $P_{cysK}::gfp$ reporter plasmid grown in sulfate-replete minimal medium with 1 mM cysteine. Strains are TIM313 (WT), TIM410 ($\Delta cysB$), TIM409 (*cysB*⁺) and TIM411 (*cysBA227D*). Gene expression was determined by normalizing the green fluorescence of an individual culture sample with its corresponding OD₆₀₀ (a.u. = arbitrary units). Each point represents an independent biological replicate, and the bar represents the mean ($n = 3$). The dotted line indicates the background level of normalized fluorescence for a non-fluorescent control (pVSV105/ES114). One-way ANOVA revealed significant differences among means ($F_{3,8} = 127.3$, $p < 0.0001$). A Dunnett's *post-hoc* test was performed to statistically compare the means of each mutant group to the mean of the wild-type group, with p -values adjusted for multiple comparisons (**** = $p < 0.0001$; n.s. = not significant with $p \geq 0.05$). Experiment was performed three times with similar results obtained among each trial.

determine whether CysBA227D enables growth on various sulfur sources, we examined the growth yield of the *cysBA227D* mutant using the panel of sulfur compounds that wild-type cells can utilize (Fig. 1). Similar to the $\Delta cysB$ mutant, the *cysBA227D* mutant could grow on cysteine and glutathione, but not on thiosulfate or sulfate (data not shown and Fig. 6A), with the latter result suggesting that the *cys* genes are not expressed sufficiently in this mutant for sulfate assimilation. However, the *cysBA227D* mutant did grow on 0.5 mM cystine (Fig. 6A), which suggests that the CysB regulon was sufficiently induced for growth on this organic sulfur source. The *cysBA227D* mutant grew similarly to wild type for cystine levels of at least 166 μ M

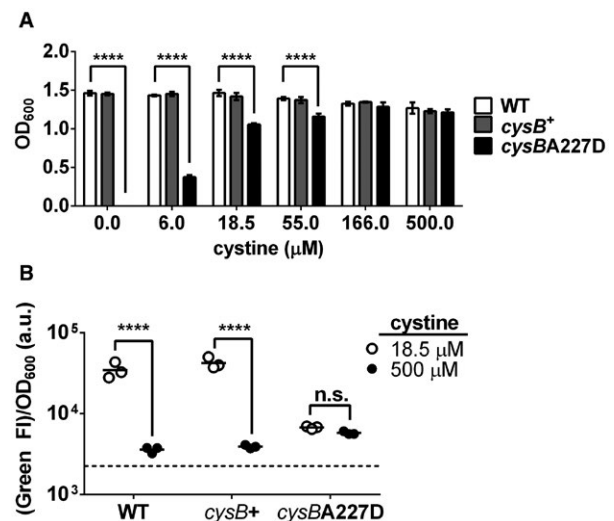


Fig. 6. Impact of *cysBA227D* on growth of *V. fischeri* in cystine. A. Growth yield of *V. fischeri* strains after 21 h of incubation in sulfate-replete media supplemented with the indicated level of cystine. Strains tested were WT = TIM313 (white), *cysB*⁺ = TIM409 (gray) and *cysBA227D* = TIM411 (black). Each bar represents the mean growth yield ($n = 3$), and error bars represent the standard deviation. Two-way ANOVA revealed significant differences among means due to cystine concentration ($F_{5,36} = 160.9$, $p < 0.0001$), genotype ($F_{2,36} = 1474$, $p < 0.0001$) and their interaction ($F_{10,36} = 296.6$, $p < 0.0001$). A Dunnett's *post-hoc* test was performed to statistically compare the means of each mutant to wild type for each concentration of cystine, with p -values adjusted for multiple comparisons (**** = $p < 0.0001$; comparisons with $p \geq 0.05$ are considered not significant and are not labeled). Experiment was performed three times with similar results obtained among each trial. B. Expression of *cysK* in indicated *V. fischeri* strains grown in low (18 μ M) or high (500 μ M) concentrations of cystine. Strains tested were same as in panel A but harbored P_{cysK} reporter plasmid pVF_1893P. Gene expression was determined by normalizing the GFP fluorescence with OD₆₀₀. Each point represents an independent biological replicate, and the bar represents the mean ($n = 3$). Two-way ANOVA revealed significant differences among means due to cystine concentration ($F_{1,12} = 136.8$, $p < 0.0001$), genotype ($F_{2,12} = 25.69$, $p < 0.0001$) and their interaction ($F_{2,12} = 32.53$, $p < 0.0001$). A Sidak's *post-hoc* test was performed to statistically compare for each strain the means between cystine concentrations, with p -values adjusted for multiple comparisons (**** = $p < 0.0001$; comparisons with $p \geq 0.05$ are considered not significant and are not labeled). Experiment was performed three times with similar results obtained among each trial.

(Fig. 6A), and significant growth of the *cysBA227D* could be detected at 6 μM (Fig. 6A). In an attempt to determine how *V. fischeri* acquires extracellular cystine, genes predicted to encode factors involved in cystine transport were targeted for deletion. In *E. coli*, deletion of *tcyJ*, which encodes a periplasmic cystine-binding protein, and *tcyP*, which encodes a symporter with lower affinity for cystine, results in a growth defect on cystine (Chonoles Imlay *et al.*, 2015). However, a *V. fischeri* mutant containing deletion alleles for both genes was able to grow on cystine (Fig. S5), suggesting that *V. fischeri* has an additional mechanism to access environmental cystine.

Based on the growth yields described above, we hypothesized that transcriptional induction of *cys* genes by CysB is necessary for normal growth on cystine levels below 166 μM . To test this hypothesis, we examined *cysK* expression in cells grown in sulfate-replete medium containing 18.5 μM (low) and 500 μM (high) cystine. Under conditions of low-cystine, wild-type levels of *cysK* expression were high (Fig. 6B), consistent with cells having exhausted cystine and then growing by assimilating sulfate. The level of *cysK* expression was 24.3 ± 4.7 times lower in media supplemented with high-cystine (Fig. 6B), suggesting that transcriptional induction by CysB is lower in this condition. This result is consistent with the reduction of cystine to two molecules of cysteine within the cytoplasm that promotes feedback inhibition on CysE and, consequently, lower levels of NAS inducer. In the *cysBA227D* mutant, the level of *cysK* expression decreased only 1.3-fold between the conditions of low- and high-cystine concentrations (Fig. 6B), suggesting that CysB mediates the transcriptional response of *cysK* to cystine. In addition, the level of *cysK* expression in the *cysBA227D* mutant was lower than that of wild type for 18.5 μM cystine but higher for 500 μM (Fig. 6B), suggesting that CysBA227D induces expression of *cys* genes to an intermediate level. Taken together with the growth yield experiments described above, these results suggest that the induction of the CysB regulon by the CysBA227D variant is sufficient to support growth on cystine but not sulfate.

The ability of the *cysBA227D* mutant to grow on cystine but not sulfate (Fig. 6A) provided a tool to investigate whether such growth properties contribute to symbiosis establishment. Animals exposed to the *cysBA227D* mutant showed luminescence and CFU levels comparable to animals colonized by the wild-type strain (Fig. S6A and B), suggesting that the CysBA227D variant enables the *V. fischeri* cells to grow within the light organ. The experimental setup associated with this result is also noteworthy because like the ΔcysB mutant, the *cysBA227D* mutant decreases in abundance within FSSW (data not shown); however, increasing the initial level of the *cysBA227D* mutant was unnecessary for the strain to establish symbiosis. These results suggest that *V. fischeri*

can grow *in vivo* on a sulfur source aside from sulfate in a manner that depends on CysB.

Differential expression of P_{cysK} within the light organ

The findings above suggest that CysB promotes growth of *V. fischeri* on a sulfur source other than sulfate *in vivo*. Because CysB functions as a transcription factor, a prediction of this model is that CysB-regulated genes will be transcriptionally induced within the host. To test this prediction, the fluorescence-based reporter system for promoter activity (Fig. 4B) was used to quantify gene expression levels of the *V. fischeri* populations occupying the various crypt spaces within the light organ, in a manner similar to a previous report (Sun *et al.*, 2015). The pTM267 vector used to clone the reporter constructs also contains *mCherry* downstream of a copy of the *tetA* promoter (Fig. 7A), which is expressed in *V. fischeri* (Miyashiro *et al.*, 2010). The mCherry fluorescence provides both a means to locate the populations of *V. fischeri* and to normalize the corresponding levels of GFP fluorescence *in vivo* (Sun *et al.*, 2015), which may be affected by factors other than promoter activity, such as population size.

Initial experiments revealed that animals exposed to an inoculum of wild-type cells harboring the P_{cysK} reporter plasmid frequently exhibited higher levels of GFP fluorescence in the *V. fischeri* populations located within the crypt spaces further from the midline of the light organ, i.e. Crypts 2 and 3 (Fig. 7A), which suggests that P_{cysK} is expressed to levels higher within those crypt spaces relative to populations within Crypt 1. Because our previous method for quantifying gene expression averaged across all of the bacteria throughout the light organ (Sun *et al.*, 2015), we modified this method to quantify gene expression within individual populations (Fig. 7B and C). First, to locate each *V. fischeri* population within an image set, the region of mCherry-positive pixels was labeled according to its corresponding crypt space (Fig. 7B). For each pixel within the region, the corresponding GFP and mCherry fluorescence levels were used to calculate a GFP/mCherry fluorescence ratio, which yielded a distribution of ratios that represents the expression of *cysK* throughout that population (Fig. 7C). Each distribution exhibited a single peak that was then fit to a Gaussian curve described by the parameters μ_{crypt} and σ_{crypt} , which correspond to the peak position and spread of GFP/mCherry ratios respectively (Fig. 7C, inset) and could be used to compare distributions.

For each crypt type, the μ_{crypt} values for *cysK* expression among the group of animals did not follow a normal distribution (Fig. 7D, Shapiro–Wilk, $\alpha = 0.05$, $p > 0.05$), suggesting that *cysK* is expressed to different levels in the populations that were established within the animal group. Despite this variability among animals, differences

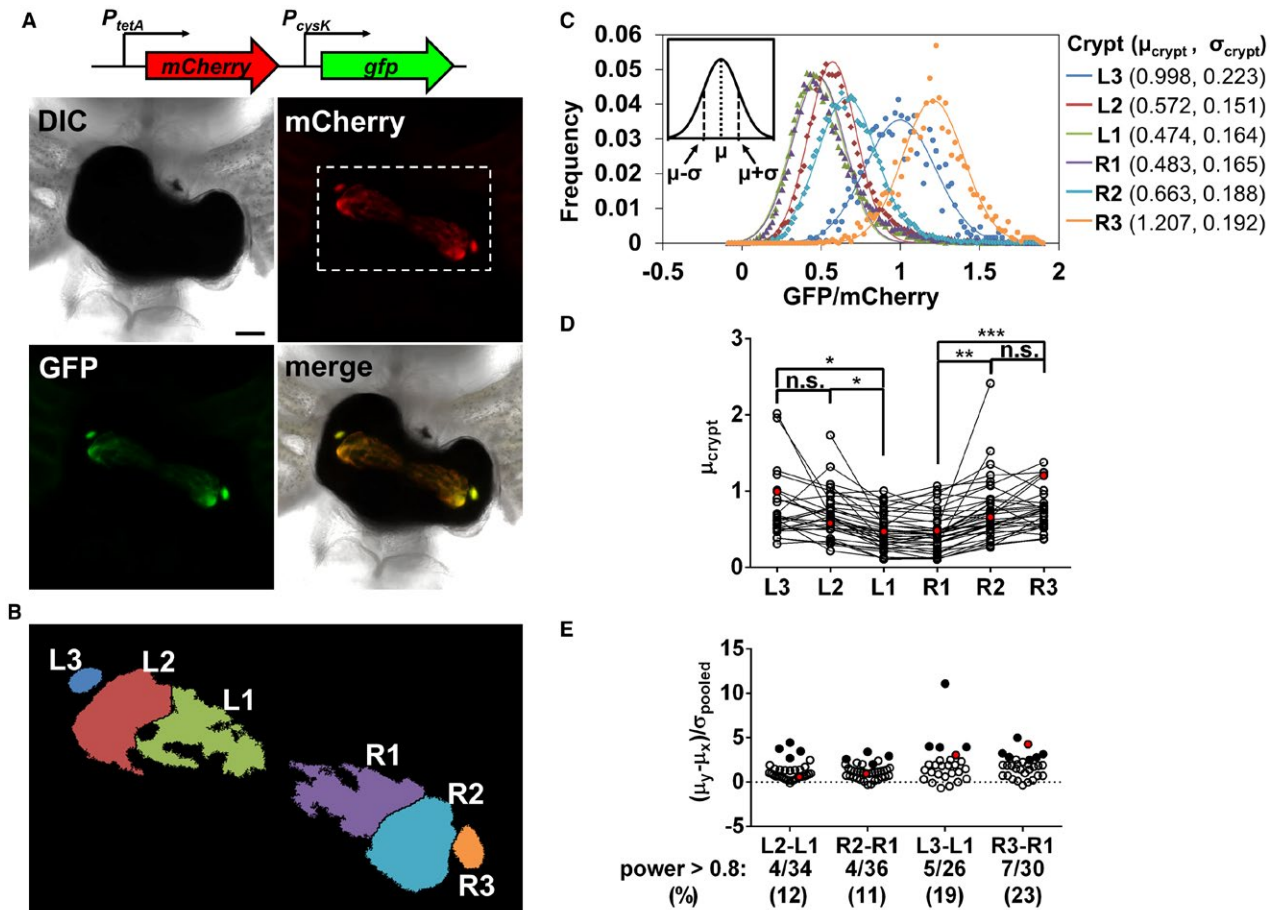


Fig. 7. Impact of location on expression of *cysK* for *V. fischeri* populations *in vivo*.

A. Above, reporter construct in plasmid pVF_1893P for measuring *cysK* expression *in vivo*. Not shown are two transcriptional terminators that are present downstream of mCherry. Below, images of a light organ from an experiment with juvenile squid ($n = 37$) exposed to an inoculum containing the WT ES114 strain harboring the P_{cysK} reporter plasmid pVF_1893P. Scale bar = 100 μ m.

B. Regions of interest corresponding to the individual populations that are each labeled according to light organ side (L or R) and crypt type (1–3). The example corresponds to the region indicated by the dotted box in the mCherry panel in A.

C. Histograms of GFP/mCherry values for pixels of individual populations identified in B. Each distribution (points) is fitted by a Gaussian curve (line), which yields parameters μ and σ (inset). Parameter values for each infection are shown to the right.

D. Levels of *cysK* expression for individual populations. Each point represents μ_{crypt} for an individual population. Lines connecting points indicate populations were within the same animal. Statistical analysis by a Kruskal–Wallis test found significant differences in mean ranks ($H = 34.49$, 5 d.f., $p < 0.0001$). A Dunn's *post-hoc* analysis was performed to statistically compare the mean ranks between crypt spaces, with p -values adjusted for multiple comparisons (n.s. = not significant, * = $p < 0.05$, ** = $p < 0.01$, *** = $p < 0.001$). Not shown for clarity: L3–R3, L2–R2 and L1–R1, which were n.s., and comparisons between populations located in crypts on different sides of the light organ, which were similar to same-side comparisons. Red points represent the populations within the light organ shown in A.

E. Comparisons of *cysK* expression distributions between populations within individual light organs. Each point represents the standardized mean difference between the indicated populations. Closed symbols represent comparisons that are significant ($\alpha = 0.05$, power > 0.8). Red points represent comparisons involving the populations within the light organ shown in A. Experiment was performed twice with similar results obtained from both trials.

were detected within the group between the μ_{crypt} values of populations within Crypt 1 relative to populations in Crypts 2 and 3 (Fig. 7D). In contrast to P_{cysK} , the μ_{crypt} values for animals colonized with wild-type cells harboring the P_{tetA} reporter exhibited normal distributions for each crypt type across the group and no difference between crypts (Fig. S7), suggesting that the observed differences in P_{cysK} expression are specific to that promoter and that the ratio calculations are not intrinsically noisy. To further characterize this pattern of gene expression,

we investigated the difference between these crypt types in individual animals by calculating (i) the magnitude of separation between the peaks of each distribution (the standardized mean difference or $(\mu_Y - \mu_X) / \sigma_{pooled}$) and (ii) the extent to which the distributions are separate (power). In the latter analysis, given two Gaussian distributions (X and Y , with $\mu_Y > \mu_X$), the differences between X and Y are deemed significant if at least 80% of Y is greater than 95% of X , i.e. power > 0.8 at $\alpha = 0.05$. For the light organ shown in Fig. 7A, the standardized mean difference

between the GFP/mCherry distributions for R3 and R1 is 4.27 with a power of 0.99 (Fig. 7D), suggesting that *cysK* expression is significantly higher in R3 than in R1. Using this analysis, we observed that 32% of squid (12/37) had at least one population within Crypt 2 or Crypt 3 exhibiting higher levels of *cysK* expression relative to the population in Crypt 1 (Fig. 7E). Over time, this pattern of differential

expression among populations becomes more frequent and exhibits larger differences between crypt spaces (Fig. S8), suggesting that the difference between crypt spaces increases as the symbiosis matures. In addition, the frequency of the expression pattern and the differences in expression were lower in animals exposed to an inoculum at a later time point (Fig. S9), suggesting that the duration

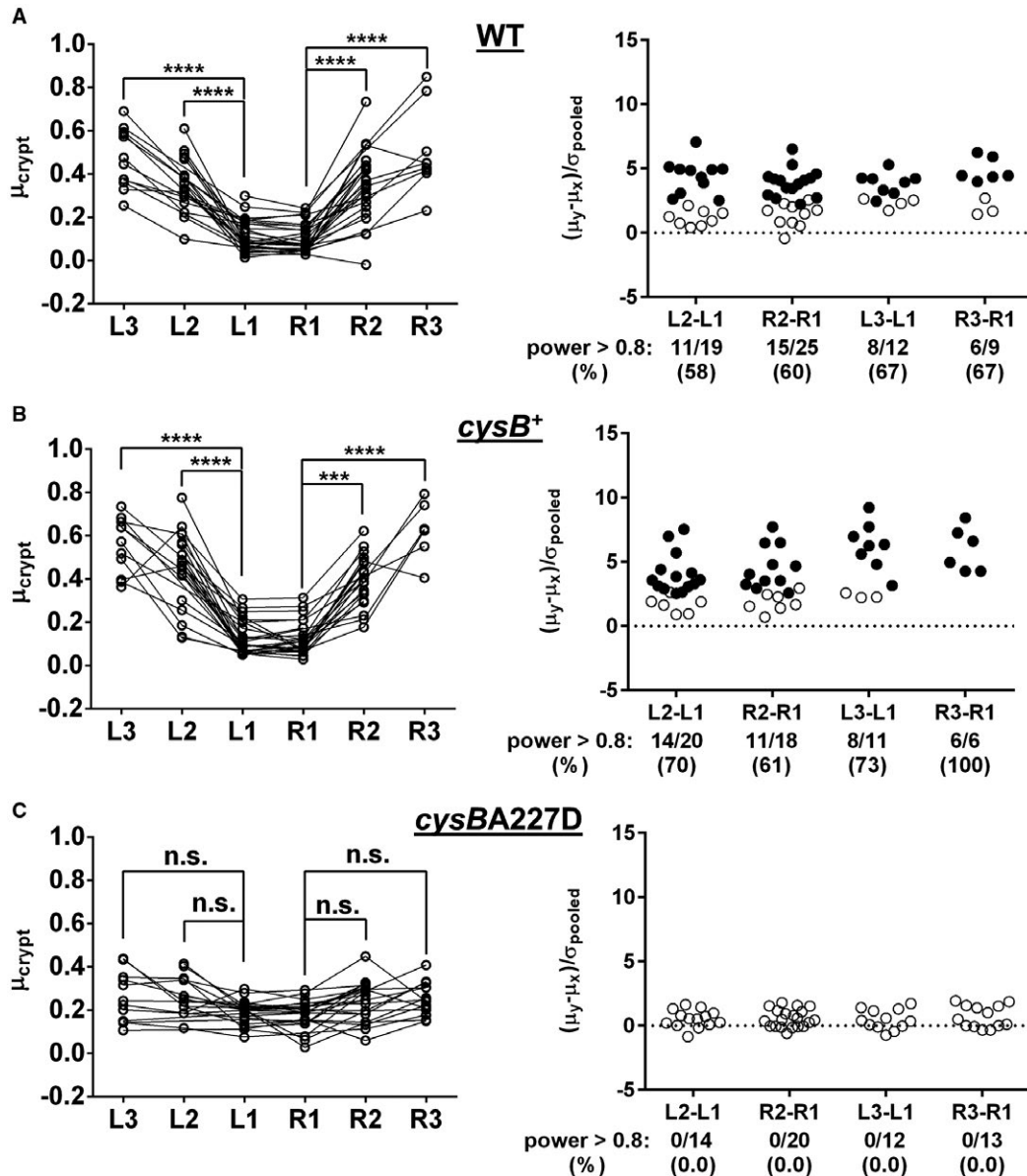


Fig. 8. Impact of CysB on expression of *cysK* in the light organs. Values of μ_{crypt} for GFP/mCherry distributions (*left*) and comparisons of GFP/mCherry distributions (*right*) at 72 h for animals colonized by the indicated strain harboring the *cysK* reporter plasmid. Each experiment involved three groups of animals ($n = 24\text{--}28$) exposed to the indicated strain. Data were analyzed statistically as described in Fig. 7 legend. For data shown in the left panels, the Kruskal–Wallis test results are listed below and a Dunn’s *post-hoc* analysis was performed to statistically compare the mean ranks between crypt spaces, with p -values adjusted for multiple comparisons (n.s. = not significant, *** = $p < 0.001$, **** = $p < 0.0001$). In right panels, closed symbols represent comparisons that are significant ($\alpha = 0.05$, power > 0.8). Experiment was performed twice with similar results obtained among both trials.

A. WT = TIM313. ($H = 79.54$, d.f. = 5, $p < 0.0001$).

B. *cysB*⁺ = TIM409. ($H = 75.36$, d.f. = 5, $p < 0.0001$).

C. *cysBA227D* = TIM411 ($H = 14.72$, d.f. = 5, $p = 0.0116$).

of the symbiotic associations is a factor in the development of the pattern of P_{cysK} expression *in vivo*. Finally, we observed the expression patterns for other CysB-regulated genes are similar to that of P_{cysK} (Fig. S10), suggesting that the crypt environments vary in a manner that impacts how CysB regulates gene expression.

Impact of CysB on gene expression *in vivo*

Our results described above suggest that CysB-regulated genes are differentially regulated among the crypts spaces within the light organ. To test whether this pattern of gene expression depends on CysB, the expression of P_{cysK} was examined in animals colonized by the *cysBA227D* mutant. At 72 h p.i., the frequency of *cysBA227D* populations for each crypt type was comparable to that for the WT strain (Fig. S11), suggesting that the altered regulation of CysB-regulated genes by CysBA227D did not impair the ability of *V. fischeri* to first access and then grow within each crypt type. Animals containing WT or *cysB*⁺ cells generally exhibited higher activity of the *cysK* promoter in Crypts 2 and 3 relative to Crypt 1 (Fig. 8A and B), which is consistent with the observed differential expression of *cysK* described above. In contrast, *cysK* expression in *cysBA227D* populations within Crypts 2 and 3 were comparable to Crypt 1 (Fig. 8C), suggesting

that the ability of CysB to regulate transcription is necessary for the pattern of differential expression of *cys* genes among the light organ populations. Comparison of the levels of P_{cysK} expression across groups according to crypt type revealed that *cysBA227D* populations exhibit lower P_{cysK} expression than wild-type for populations within Crypts 2 and 3, but higher expression of P_{cysK} in Crypt 1 (Fig. 8A–C). These results suggest that CysB induces *cys* gene expression in the populations within the distal crypts but does not induce expression of *cys* genes in Crypt 1 populations.

Discussion

The fitness of a horizontally transmitted microbe *in vivo* depends on its access to nutrients within host-associated niches. In this study, the symbiotic bacterium *V. fischeri* was used to explore the molecular mechanisms to acquire sulfur for growth during the initial colonization of the squid light organ. While *V. fischeri* can grow on multiple sulfur sources (Fig. 1), the ability to grow on cystine was associated with establishing symbiosis (Figs 6A and S6). This growth property is controlled by the transcription factor CysB (Fig. 6A), which, through gene regulation, is predicted to modulate the intracellular cysteine pools that serve as the primary source of sulfur for

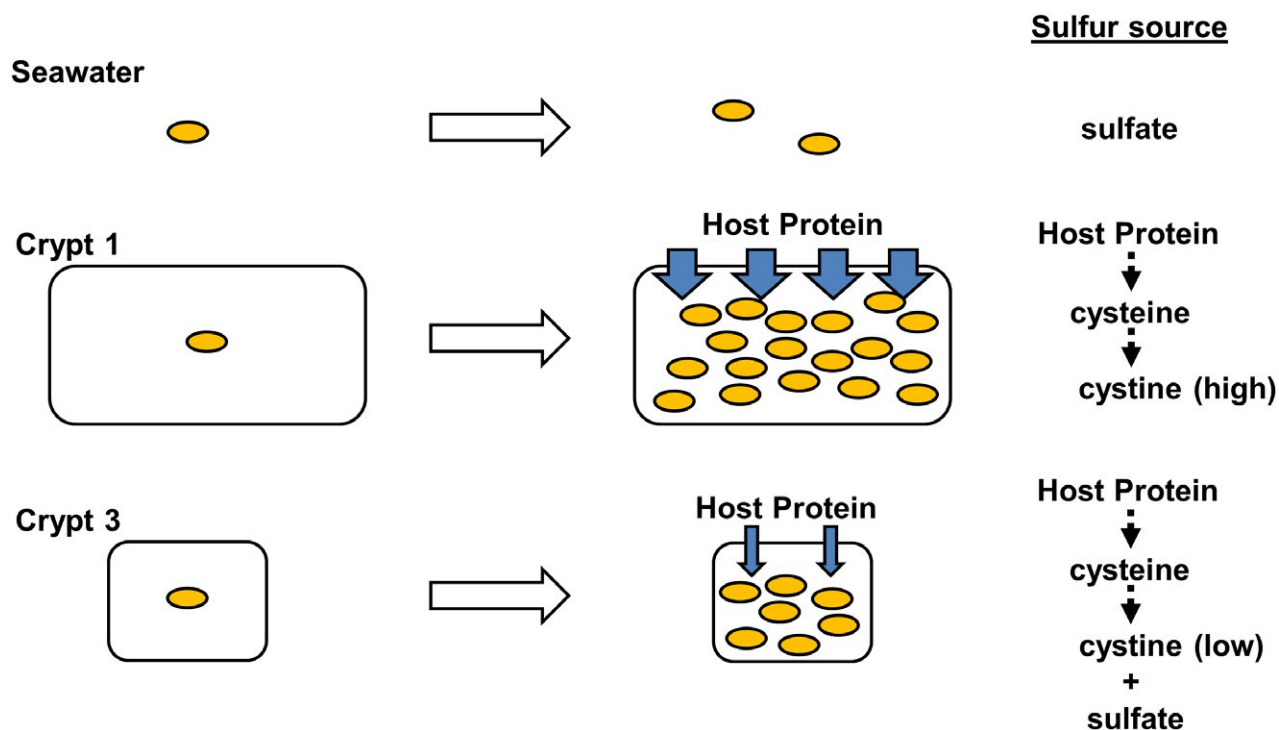


Fig. 9. Model of sulfur acquisition by *V. fischeri* during symbiosis. Growth of *V. fischeri* in seawater (top) is restricted to sulfate assimilation. For cells that enter Crypt 1, growth is mediated by host-derived compounds, e.g. host protein. Upon degradation of these proteins, cysteine residues are released and undergo auto-oxidation to cystine, which *V. fischeri* uses as a sulfur source. In Crypts 2 and 3, the concentration of bioavailable cystine is lower, which results in *V. fischeri* satisfying its sulfur requirements for growth through sulfate assimilation.

anabolic processes (Kredich, 1996). Furthermore, growth on cystine results in decreased expression of cysteine biosynthesis genes relative to sulfate conditions (Fig. 6B), consistent with cells lowering *de novo* synthesis of cysteine due to the availability of a compound that can contribute to cysteine pools within the cytoplasm. The finding of different levels of transcriptional induction by CysB among the populations that occupy different crypt types (Fig. 8) suggests that *V. fischeri* modulates cysteine biosynthesis in accordance with the availability of nutrients within each colonization site *in vivo*.

The results obtained during this study have led to the model for acquisition of sulfur by *V. fischeri* during symbiosis establishment proposed in Fig. 9. While outside of the host, *V. fischeri* grows on sulfate that is readily available in seawater. This sulfur is converted into an organic form through the biosynthesis of cysteine, which is subsequently available for anabolism. However, when a *V. fischeri* cell enters a crypt space within the light organ, it gains access to host-derived proteins. Proteolysis of these proteins releases a plethora of amino acids into the crypt spaces. Cleaved cysteine residues autoxidize; resulting in the formation of cystine that is sufficient for CysB-dependent growth of *V. fischeri* within the crypt space. While *V. fischeri* may grow on the same type of sulfur source within every crypt space (i.e. host-derived proteins), its availability appears to vary among each type of crypt space, with the lowest concentration present in Crypt 3. Growth on these host-derived nutrients within the crypt spaces establishes the populations that produce bioluminescence during symbiosis.

The solubility of cystine at physiological ranges of pH suggest it is possible for cystine to be available within the crypt spaces. While the compounds that specifically facilitate *V. fischeri* growth *in vivo* are unknown, proteomic analysis of the crypt contents in light organs of adult animals has revealed that *V. fischeri* is exposed to numerous host proteins *in vivo* (Schleicher and Nyholm, 2011), which may serve as a source of peptides and amino acids for bacterial growth. A particularly intriguing candidate is hemocyanin, which is a metalloprotein that is expressed in the gills and hypothesized to shuttle oxygen from the gills to the light organ crypt spaces (Kremer *et al.*, 2014), where oxygen serves as a substrate for the light-producing enzyme luciferase. The hemocyanin isoforms of *E. scolopes* contain numerous cysteines that are predicted to form at least 22 disulfide bonds that contribute to the structure necessary for oxygen carriage (Kremer *et al.*, 2014). If released through degradation and then auto-oxidized, these cysteine residues may serve as an abundant source of sulfur for bacterial growth *in vivo*. Alternatively, other host-derived factors, such as sulfated glycoproteins or small molecules, may also contribute to the growth of *V. fischeri* within the light organ. The results

presented here warrant future investigation into the growth of *V. fischeri* on particular host-derived compounds found in the crypt spaces.

Elucidating the mechanisms that enable *V. fischeri* to grow on cystine *in vitro* will likely provide insight into the sulfur sources that promote *V. fischeri* growth within the crypt spaces. The disruption of two genes predicted to each facilitate cystine transport failed to prevent growth of *V. fischeri* on cystine (Fig. S5), suggesting that *V. fischeri* has at least one other mechanism for uptake of environmental cystine. Another direction for future studies includes determining the extent to which *V. fischeri* actively degrades compounds within the host environment to release nutrients for growth. *V. fischeri* encodes multiple aminopeptidases that may contribute to the degradation of host proteins, with PepN responsible for the majority of aminopeptidase activity observed *in vitro* (Fidopiastis *et al.*, 2012). This aminopeptidase activity was primarily associated with cells rather than cell-free supernatant (Fidopiastis *et al.*, 2012), suggesting that PepN may contribute to breaking down peptides that have been taken up by the cells expressing PepN. Within the squid, the abundance of a *pepN* mutant is initially reduced relative to wild-type cells but then achieves normal levels by 24 h p.i. (Fidopiastis *et al.*, 2012), suggesting PepN activity may contribute to growth *in vivo*. Four other aminopeptidases are upregulated by 3-oxo-C6 HSL (Antunes *et al.*, 2007), which promotes bioluminescence production by *V. fischeri* populations within the squid light organ. The expression of these genes through quorum sensing may permit *V. fischeri* cells to coordinate the expression of aminopeptidases with cell density within each crypt space, thereby optimizing the release of amino acids from host-derived proteins for the amount of cells present within a population. Future studies are necessary to examine any link between aminopeptidase activity of *V. fischeri* and the response of CysB *in vivo*.

The striking heterogeneity in the expression of CysB-regulated genes observed for populations in different crypt types provides further evidence that the specific environment experienced by a *V. fischeri* population depends on the particular crypt that is colonized. Recently, a fluorescence-based reporter derived from PhoB-regulated genes was used as a biosensor for phosphate availability *in vivo* (Stoudenmire *et al.*, 2018). Fluorescence-based microscopy of the light organs colonized by *V. fischeri* harboring this reporter revealed heterogeneity in expression (i) among animals, (ii) among crypt spaces in the same animal and (iii) even across individual populations, suggesting that phosphate availability *in vivo* follows a complex spatiotemporal profile that may be linked to host development. The inferred variation in phosphate within individual populations was not observed for the conditions that stimulate CysB-dependent gene expression,

suggesting that the spatial profiles for each process are different. Variation among the crypt spaces impacts the population structure during symbiosis establishment, as populations of non-luminescent strains that initially form in Crypt 1 fail to be maintained (Verma and Miyashiro, 2016). The specific conditions within each crypt type may provide selective pressure that contributes to the genetic variability observed among strains isolated from wild-caught animals (Wollenberg and Ruby, 2009; Sun *et al.*, 2016). Further characterization of the habitat environments within the light organ will enable the testing of hypotheses associated with the adaptation of particular strains *in vivo*.

This study included the quantification of gene-expression profiles of individual populations *in situ*. CysB is conserved in other bacteria, including the pathogen *Pseudomonas aeruginosa*, which was recently shown to use it to regulate transcription of the PqsR receptor that controls expression of virulence factors (Farrow *et al.*, 2015). Further investigation into the CysB regulon of *P. aeruginosa* may reveal the extent to which cellular responses to sulfur availability impacts its pathogenicity. More generally, approaches based on the biogeography of bacteria within the host will be important for uncovering the mechanisms that impact microbial fitness within host-associated niches. For instance, investigation of *Vibrio cholerae* cells within the infant-mouse infection model revealed the presence of microcolonies localized to the crypt spaces of proximal small intestine (Millet *et al.*, 2014). However, within the distal region of the small intestine, the cells were not limited only to the crypt spaces. Learning how *V. cholerae* grows within these different sites may lead to the development of novel therapeutics designed to specifically target *V. cholerae* within the host. The exclusive nature of the squid-*Vibrio* association and the well-defined niches for bacterial populations within the light organ have led to the discoveries that the ability to grow on cystine is an important trait for *V. fischeri* to grow *in vivo* and that the host-derived sulfur source varies among colonization sites. These findings will serve as the foundation for future investigations into the mechanisms bacterial symbionts use to grow within their hosts.

Experimental procedures

Media and growth conditions

V. fischeri strains were grown aerobically at 28°C in LBS medium [1% (wt/vol) tryptone, 0.5% (wt/vol) yeast extract, 2% (wt/vol) NaCl, 50 mM Tris-HCl (pH 7.5)], defined-minimal medium (DMM) [50 mM MgSO₄, 10 mM CaCl₂, 300 mM NaCl, 10 mM KCl, 0.0058% (wt/vol) K₂HPO₄, 10 μM FeSO₄, 50 mM Tris-HCl (pH 7.5)] containing 10 mM GlcNAc, or sulfur-free DMM [50 mM MgCl₂, 10 mM CaCl₂,

Table 1. Strains and plasmids used in this study.

Strains	Genotype	Reference
ES114	wild-type <i>V. fischeri</i>	Ruby <i>et al.</i> (2005)
SCV001	ES114 $\Delta tcyJ$	This study
NPW003	ES114 $\Delta cysB$	This study
NPW056	ES114 $\Delta tcyJ \Delta tcyP$	This study
EVS102	ES114 $\Delta luxCDABEG$	Bose <i>et al.</i> (2008)
KL173	ES114 <i>cysD::Tn5</i>	This study
KL174	ES114 <i>cysK::Tn5</i>	This study
KL175	ES114 <i>cysJ::Tn5</i>	This study
TIM313	ES114 Tn7::[erm]	Miyashiro <i>et al.</i> (2010)
TIM409	ES114 $\Delta cysB$ Tn7::[<i>cysB erm</i>]	This study
TIM410	ES114 $\Delta cysB$ Tn7::[erm]	This study
TIM411	ES114 $\Delta cysB$ Tn7::[<i>cysBA227D erm</i>]	This study
Plasmids	Genotype	Reference
pEVS79	pBC SK (+) <i>oriT cat</i>	Stabb and Ruby (2002)
pEVS104	R6Kori RP4 <i>oriT trb tra kan</i>	Stabb and Ruby (2002)
pEVS107	R6Kori <i>oriT mini-Tn7 mob erm kan</i>	McCann <i>et al.</i> (2003)
pTM267	pVSV105 P _{tetA} - <i>mCherry kan::gfp</i>	Miyashiro <i>et al.</i> (2010)
pLosTfoX	pEVS79 <i>tfoX</i>	Pollack-Berti <i>et al.</i> (2010)
pTM392	pEVS79 $\Delta tcyJ$	This study
pNW008	pEVS79 $\Delta ydjN$	This study
pTM417	pEVS79 $\Delta cysB$	This study
pTM420	pEVS107 <i>cysB</i>	This study
pTM423	pEVS107 <i>cysBA227D</i>	This study
pSCV26	pTM267 Δkan P _{tetA} - <i>gfp</i>	This study
pUX-BF13	R6Kori <i>tns bla</i>	Bao <i>et al.</i> (1991)
pVF_0008P	pTM267 Δkan P _{tcyJ} - <i>gfp</i>	This study
pVF_0310P	pTM267 Δkan P _{cysJ} - <i>gfp</i>	This study
pVF_0320P	pTM267 Δkan P _{cysD} - <i>gfp</i>	This study
pVF_1893P	pTM267 Δkan P _{cysK} - <i>gfp</i>	This study
pVSV105	R6Kori <i>ori</i> (pES213) RP4 <i>oriT cat</i>	Dunn <i>et al.</i> (2006)

300 mM NaCl, 10 mM KCl, 0.0058% (wt/vol) K₂HPO₄, 10 μM FeCl₃, 50 mM Tris-HCl (pH 7.5)] containing 10 mM GlcNAc. To maintain plasmids, chloramphenicol was added to the medium at a final concentration of 2.5 μg ml⁻¹. Strains that are cysteine auxotrophs were propagated with 1 mM cysteine.

Strains

All *V. fischeri* strains used in this study are listed in Table 1 and were derived from ES114 (Ruby *et al.*, 2005).

Construction of deletion alleles. The deletion alleles $\Delta cysB$, $\Delta tcyJ$ and $\Delta tcyP$ were individually constructed by amplifying from ES114 genomic DNA by PCR ~1.5 kb on either side of the corresponding gene and cloning the products into

Table 2. Primers used in this study.

Primer name	Sequence (5' ≥ 3')
<i>Deletion alleles</i>	
<i>ΔcysB</i>	
<i>ΔcysB</i> -5-Sall-u	GGGTCGACGGATCAGCGTGGTGTGCCATTATCA
<i>ΔcysB</i> -5-XbaI-l	GCTCTAGACTCAGCAGTCGATGATACATTCAA
<i>ΔcysB</i> -3-XbaI-u	GCTCTAGATAAGATCGCCCTGATATTATTTTC
<i>ΔcysB</i> -3-SacI-l	GGGAGCTCGGTATGTTCTCTTTCTCTGGTCTT
<i>ΔtcyJ</i>	
<i>ΔtcyJ</i> -5-XbaI-u	GGTCTAGAGTTCCTTGTTCGACGATCTTTCCA
<i>ΔtcyJ</i> -5-XmaI-l	GGCCCGGGGATTACTCACCATTCATCAAATAA
<i>ΔtcyJ</i> -3-XmaI-u	GGCCCGGGGATTAGGATGATACTTTTTTTTGC
<i>ΔtcyJ</i> -3-EcoRV-l	GGGATATCGCATTCGCAATAACACGATTTAAT
<i>ΔtcypP</i>	
<i>ΔtcypP</i> -5-Sall-u	GGGTCGACGATTACCTAACACCCAAATATCAT
<i>ΔtcypP</i> -5-HindIII-l	CCGAAGCTTTACGTTGCTGTGTATTAATAAAAAAG
<i>ΔtcypP</i> -3-HindIII-u	GGTAGAAAGCGCACAAAGCTTAAT
<i>ΔtcypP</i> -3-SacI-l	GGGAGCTCGTGCTATACGAGATGTTATTACTC
<i>cysB alleles</i>	
<i>cysB</i> ⁺	
<i>cysB</i> ⁺ -KpnI-u	GGGGTACCGTAGTAATATTTTCCAGTGTAAACA
<i>cysB</i> ⁺ -SpeI-l	GGACTAGTGGTCTATATTTAAAAACTGCTGAG
<i>cysBA227D</i>	
<i>cysBA227D</i> -u	GTCTTTACCGCAACCGATGATGATGTCATTAAGACTTATG
<i>cysBA227D</i> -l	CATAAGTCTTAATGACATCATCATCGGTTGCGGTAAGAC
<i>Promoter reporters</i>	
<i>P</i> _{tcyJ} -XmaI-u	GGCCCGGGGAAGCCAAAGCGATGAAGACACGG
<i>P</i> _{tcyJ} -XbaI-l	GGTCTAGAGCGAGGATATTCCTTCGTCCATTTC
<i>P</i> _{cysD} -XmaI-u	GGCCCGGGGAGAGGTTTCATAGTGTCTCCAAA
<i>P</i> _{cysD} -XbaI-l	GGTCTAGATTGCTGAAGGTGGGTCAATCGTTT
<i>P</i> _{cysJ} -XmaI-u	GGCCCGGGGGTAAGAATCAACGAATAAACGAT
<i>P</i> _{cysJ} -XbaI-l	GGTCTAGAGAGAGTTCCCTTAATAACATGACG
<i>P</i> _{cysK} -XmaI-u	GGCCCGGGGATGTTTACCGTGATACACATAAA
<i>P</i> _{cysK} -XbaI-l	GGTCTAGAGAGAATTATCTTCGTAAATCTTTG
<i>P</i> _{tetA} -XmaI-XbaI-u	CCGGGTTGACACTCTATCATTGATAGAGTTATTTTACCACTCGCT
<i>P</i> _{tetA} -XmaI-XbaI-l	CTAGAGCGAGTGGTAAAATAACTCTATCAATGATAGAGTGTCAACTC

pEVS79 to yield plasmids pTM417, pTM392 and pNW008 respectively. Primers and restriction sites are listed in Table 2. To construct a mutant with a particular deletion allele, the corresponding plasmid containing the deletion allele was introduced into a target strain by conjugation using pEVS104 (Stabb and Ruby, 2002) and screening for a double-cross-over event, as described elsewhere (Miyashiro *et al.*, 2010).

Construction of *cysB*⁺ and *cysBA227D* alleles. To generate the *cysB*⁺ strain TIM409, the gene *VF_1490* was amplified with its promoter region by PCR from ES114 genomic DNA using the primers indicated in Table 2. The resulting amplicon was cloned into pCR-Blunt (Life Technologies, Carlsbad, CA, USA) and then sub-cloned using KpnI/SpeI restriction sites into pEVS107 to yield pTM420. The *cysB*⁺ allele was integrated into the large chromosome of the *ΔcysB* strain NPW003 at the Tn7 site as described elsewhere (Miyashiro *et al.*, 2011). To generate the *cysBA227D* allele, the pCR-Blunt clone containing the *cysB*⁺ allele was used as a template for PCR-based, site-directed mutagenesis with the primer set listed in Table 2. The reaction contained PFU Ultra DNA Polymerase (Agilent Technologies,

Santa Clara, CA) with 0.2 mM dNTPs, 125 ng each primer and 20 nM plasmid template. Amplification was performed in a C1000 Thermal Cycler (Bio-Rad, Hercules, CA, USA) with the following steps: (i) 95°C/30 s, (ii) 95°C/30 s, (iii) 55°C/1 m, (iv) 68°C/10 m and (v) 18 cycles of steps 2–4. The PCR product was digested with 10 U DpnI overnight and transformed into Top10 by electroporation. The resulting *cysBA227D* was sub-cloned into pEVS107 to yield pTM423 and then integrated into the Tn7 site of NPW003 as described above.

Construction of *cys* Tn5-insertion mutants. The *cysD*::Tn5, *cysK*::Tn5 and *cysJ*::Tn5 alleles were obtained as part of a different study involving a Tn5-based screen designed to identify mutants with elevated levels of GFP in colonies using the *P*_{tcyJ} reporter plasmid pVF_0008P (Wasilko NP and Miyashiro T, unpublished). To construct mutants with clean genetic backgrounds, the alleles were introduced into ES114 using a protocol using pLosTfoX (Pollack-Berti *et al.*, 2010), which overexpresses a regulator that enables introduction of markers into strains by natural transformation (Miyashiro *et al.*, 2014).

Promoter reporter plasmids

To construct reporter plasmids, the promoter regions were amplified from ES114 genomic DNA by PCR using the corresponding primer sets listed in Table 2. The products were cloned into pCR-Blunt, verified by sequencing and isolated via digestion with XmaI/XbaI. The resulting products were subcloned into the vector fragment of pTM267 (Miyashiro *et al.*, 2010) that was digested with XmaI/XbaI. For constructing pSCV26, which contains the *tetA* promoter upstream of *gfp*, the oligonucleotides tetA-XmaI-XbaI-u-I were initially heated at 95°C for 2 min and then cooled to room temperature. The ends were phosphorylated by polynucleotide kinase (New England Biolabs, Ipswich, MA, USA) and subcloned into pTM267 as described above.

Growth yield assays

Overnight cultures were diluted 1:100 into LBS and incubated aerobically with shaking at 28°C. After 2 h, cells were normalized to OD₆₀₀ = 1 and a 1 ml of sample was centrifuged at 15,000×g. After 2 min, the supernatant was removed, and the pellets were washed twice with 1 ml of DMM (or sulfur-free DMM for assays requiring a negative control for supplementation with a sulfur source). The washed cells were diluted 1:100 into the indicated medium and incubated aerobically with shaking at 28°C. After 21 h, the OD₆₀₀ of each culture was measured with a BioPhotometer Plus (Eppendorf, Hamburg, Germany).

Culture-based gene expression assay

For gene expression measurements, cultures grown in LBS overnight were diluted 1:100 into fresh LBS medium and grown aerobically with shaking at 28°C. At OD₆₀₀ = 1.0, cultures were diluted into DMM supplemented with the indicated sulfur source and grown aerobically with shaking at 28°C. At OD₆₀₀ = 1.0, 1 ml of samples were quickly cooled on an ice-slurry. Cells were pelleted by centrifugation at 4°C for 5 min at 15,000×g and re-suspended in 350 µl of cold DMM. For each sample, three 100 µl technical replicates were measured with a Tecan M1000Pro fluorescence plate reader (Tecan Group, Männedorf, Switzerland) for OD₆₀₀ and green fluorescence (488 ± 5 nm excitation/509 ± 5 nm emission). Expression levels were determined by normalizing each green fluorescence measurement by the corresponding OD₆₀₀ measurement. The background fluorescence associated with the non-fluorescent strain pVSV105/ES114 grown in parallel was subtracted from each expression level prior to calculating fold changes between samples.

Squid colonization assays

To initiate squid colonization assays, freshly hatched juvenile squid were introduced into plastic tumblers containing filter-sterilized Instant Ocean seawater (FSSW) with inoculums ranging from 3,000–10,000 CFU/ml. At indicated time points, animals were washed by transferring to fresh FSSW. Animal luminescence was measured using a GloMax 20/20 luminometer (Promega, Madison, WI, USA).

To determine bacterial abundance in FSSW, samples were serially diluted and plated onto LBS medium supplemented with cysteine. The corresponding CFU counts were used to calculate strain abundance. To determine abundance of bacteria within squid, juvenile squid were first frozen at –80°C for at least 24 h and then homogenized. The homogenate was serially diluted for determining CFU counts as described above. For assays involving fluorescence microscopy, animals were first transferred as a group to a vial on ice. After 10 min, the anesthetized animals were fixed by exposing the animal group to cold 4% paraformaldehyde/marine phosphate buffered saline (mPBS). After 24 h, animals were washed exhaustively in mPBS, and their mantles were dissected to reveal the light organ for microscopy. While the Pennsylvania State University does not require IACUC approval for invertebrate research, the anesthetization steps described above take into account recommendations for humane care and use of laboratory animals.

To quantify fluorescence levels within host-associated populations, light organs were imaged by fluorescence microscopy using a Zeiss 780 confocal microscope (Carl Zeiss AG, Jena, Germany) equipped with a 10× water lens and confocal pinholes set at maximum to mimic quantitative epi-fluorescence conditions. DIC, GFP and mCherry 12-bit images were collected and processed using the following image-analysis protocol. To identify the location of bacterial populations within the image sets, the mCherry fluorescence images were subjected to thresholding in ImageJ software, version 1.47 (NIH). Populations were defined as particles larger than 100 pixels, and when necessary, a 3-pixel-wide line was drawn to distinguish the infections. For each infection, the GFP and mCherry fluorescence levels of the corresponding pixels were determined by subtracting the background fluorescence associated with host tissue using custom Matlab scripts, version R2013a (MathWorks Inc., Natick, MA, USA). These fluorescence levels were used to calculate the GFP/mCherry fluorescence ratio for each pixel in the defined regions. The subset of GFP/mCherry fluorescence ratios within the average ± 3 standard deviations were fit to a Gaussian model $y = ae^{-\left(\frac{x-b}{c}\right)^2}$, where a , b and c are the amplitude, centroid and related to peak width, respectively, that are determined from the fitting function. The peak location (μ_{crypt}) is equal to b , and the spread (σ_{crypt}) was calculated as $c/\sqrt{2}$.

Statistical analyses

Statistical analyses were performed using Prism software (Graphpad, La Jolla, CA, USA).

Acknowledgements

This work was supported by the National Institutes of Health Grant R00 GM097032 (to T.M.) and the Pennsylvania State University Eberly College of Science. The funders had no role in study, design, data collection and interpretation, or the decision to submit the work for publication. We thank Kyle LaPenna for generating the strains KL173, KL174 and KL175 and members of the Miyashiro lab for constructive criticism of

this project. We thank the Statistical Consulting Center at Penn State University for offering advice on statistical analyses.

Conflict of interest

The authors declare no conflict of interest.

Author contributions

NPW and TM contributed to all aspects of the study, including experimental design; acquisition, analysis, and interpretation of the data and writing the manuscript. JLV and SCV contributed to the squid colonization assays, image analysis and promoter constructs. CHS contributed to the squid colonization assays and statistical analyses of the data throughout the study. BMN contributed to the acquisition, analysis and interpretation of the seawater survival and bioluminescence assays.

References

- Antunes, L.C., Schaefer, A.L., Ferreira, R.B., Qin, N., Stevens, A.M., Ruby, E.G., *et al.* (2007) Transcriptome analysis of the *Vibrio fischeri* LuxR-LuxI regulon. *Journal of Bacteriology*, **189**(22), 8387–8391.
- Bao, Y., Lies, D.P., Fu, H. and Roberts, G.P. (1991) An improved Tn7-based system for the single-copy insertion of cloned genes into chromosomes of gram-negative bacteria. *Gene*, **109**(1), 167–168.
- Bose, J.L., Rosenberg, C.S. and Stabb, E.V. (2008) Effects of *luxCDABEG* induction in *Vibrio fischeri*: enhancement of symbiotic colonization and conditional attenuation of growth in culture. *Archives of Microbiology*, **190**(2), 169–183.
- Chonoles Imlay, K.R., Korshunov, S. and Imlay, J.A. (2015) Physiological roles and adverse effects of the two cysteine importers of *Escherichia coli*. *Journal of Bacteriology*, **197**(23), 3629–3644.
- Dunn, A.K., Millikan, D.S., Adin, D.M., Bose, J.L. and Stabb, E.V. (2006) New *rfp*- and *pES213*-derived tools for analyzing symbiotic *Vibrio fischeri* reveal patterns of infection and *lux* expression in situ. *Applied and Environment Microbiology*, **72**(1), 802–810.
- Farrow, J.M. 3rd, Hudson, L.L., Wells, G., Coleman, J.P. and Pesci, E.C. (2015) CysB negatively affects the transcription of *pqsR* and *Pseudomonas* quinolone signal production in *Pseudomonas aeruginosa*. *Journal of Bacteriology*, **197**(12), 1988–2002.
- Fidopiastis, P.M., Rader, B.A., Gerling, D.G., Gutierrez, N.A., Watkins, K.H., Frey, M.W., *et al.* (2012) Characterization of a *Vibrio fischeri* aminopeptidase and evidence for its influence on an early stage of squid colonization. *Journal of Bacteriology*, **194**(15), 3995–4002.
- Gilbert, S.F., Bosch, T.C. and Ledon-Rettig, C. (2015) Eco-Evo-Devo: developmental symbiosis and developmental plasticity as evolutionary agents. *Nature Reviews Genetics*, **16**(10), 611–622.
- Graf, J. and Ruby, E.G. (1998) Host-derived amino acids support the proliferation of symbiotic bacteria. *Proceedings of the National Academy of Sciences USA*, **95**(4), 1818–1822.
- Hillen, W. and Berens, C. (1994) Mechanisms underlying expression of Tn10 encoded tetracycline resistance. *Annual Review of Microbiology*, **48**, 345–369.
- Jones, B.W. and Nishiguchi, M.K. (2004) Counterillumination in the Hawaiian bobtail squid, *Euprymna scolopes* Berry (Mollusca: Cephalopoda). *Marine Biology*, **144**, 1151–1155.
- Kredich, N.M. (1992) The molecular basis for positive regulation of *cys* promoters in *Salmonella typhimurium* and *Escherichia coli*. *Molecular Microbiology*, **6**(19), 2747–2753.
- Kredich, N.M. and Tomkins, G.M. (1966) The enzymic synthesis of L-cysteine in *Escherichia coli* and *Salmonella typhimurium*. *Journal of Biological Chemistry*, **241**(21), 4955–4965.
- Kredich, N.M. (1996) Biosynthesis of cysteine. In: Neidhardt, F.C., Curtiss, R., III, Ingraham, J.L., Lin, E.C.C., Low, K.B., Magasanik, B., *et al.* (Eds.) *Escherichia coli and Salmonella: Cellular and Molecular Biology*. Washington, DC: American Society for Microbiology, pp. 514–527.
- Kremer, N., Schwartzman, J., Augustin, R., Zhou, L., Ruby, E.G., Hourdez, S., *et al.* (2014) The dual nature of haemocyanin in the establishment and persistence of the squid-vibrio symbiosis. *Proceedings of the Royal Society B: Biological Sciences*, **281**(1785), 20140504.
- Lochowska, A., Iwanicka-Nowicka, R., Plochocka, D. and Hryniewicz, M.M. (2001) Functional dissection of the LysR-type CysB transcriptional regulator. Regions important for DNA binding, inducer response, oligomerization, and positive control. *Journal of Biological Chemistry*, **276**(3), 2098–2107.
- McCann, J., Stabb, E.V., Millikan, D.S. and Ruby, E.G. (2003) Population dynamics of *Vibrio fischeri* during infection of *Euprymna scolopes*. *Applied and Environment Microbiology*, **69**(10), 5928–5934.
- McFall-Ngai, M.J. (2014) The importance of microbes in animal development: lessons from the squid-vibrio symbiosis. *Annual Review of Microbiology*, **68**(1), 177–194.
- Meadows, J.A. and Wargo, M.J. (2014) Catabolism of host-derived compounds during extracellular bacterial infections. *Journal of Cellular Biochemistry*, **115**(2), 217–223.
- Meighen, E.A. (1993) Bacterial bioluminescence: organization, regulation, and application of the *lux* genes. *The FASEB Journal*, **7**(11), 1016–1022.
- Millet, Y.A., Alvarez, D., Ringgaard, S., von Andrian, U.H., Davis, B.M. and Waldor, M.K. (2014) Insights into *Vibrio cholerae* intestinal colonization from monitoring fluorescently labeled bacteria. *PLoS Pathogens*, **10**(10), e1004405.
- Mittal, M., Singh, A.K. and Kumaran, S. (2017) Structural and biochemical characterization of ligand recognition by CysB, the master regulator of sulfate metabolism. *Biochimie*, **142**, 112–124.
- Miyashiro, T. and Ruby, E.G. (2012) Shedding light on bioluminescence regulation in *Vibrio fischeri*. *Molecular Microbiology*, **84**(5), 795–806.
- Miyashiro, T., Wollenberg, M.S., Cao, X., Oehlert, D. and Ruby, E.G. (2010) A single *qrr* gene is necessary and

- sufficient for LuxO-mediated regulation in *Vibrio fischeri*. *Molecular Microbiology*, **77**(6), 1556–1567.
- Miyashiro, T., Klein, W., Oehlert, D., Cao, X., Schwartzman, J. and Ruby, E.G. (2011) The *N*-acetyl-D-glucosamine repressor NagC of *Vibrio fischeri* facilitates colonization of *Euprymna scolopes*. *Molecular Microbiology*, **82**(4), 894–903.
- Miyashiro, T., Oehlert, D., Ray, V.A., Visick, K.L. and Ruby, E.G. (2014) The putative oligosaccharide translocase SypK connects biofilm formation with quorum signaling in *Vibrio fischeri*. *Microbiologyopen*, **3**(6), 836–848.
- Pollack-Berti, A., Wollenberg, M.S. and Ruby, E.G. (2010) Natural transformation of *Vibrio fischeri* requires *tfoX* and *tfoY*. *Environmental Microbiology*, **12**(8), 2302–2311.
- Reid, G., Younes, J.A., Van der Mei, H.C., Gloor, G.B., Knight, R. and Busscher, H.J. (2011) Microbiota restoration: natural and supplemented recovery of human microbial communities. *Nature Reviews Microbiology*, **9**(1), 27–38.
- Ruby, E.G., Urbanowski, M., Campbell, J., Dunn, A., Faini, M., Gunsalus, R., et al. (2005) Complete genome sequence of *Vibrio fischeri*: a symbiotic bacterium with pathogenic congeners. *Proceedings of the National Academy of Sciences USA*, **102**(8), 3004–3009.
- Schleicher, T.R. and Nyholm, S.V. (2011) Characterizing the host and symbiont proteomes in the association between the Bobtail squid, *Euprymna scolopes*, and the bacterium, *Vibrio fischeri*. *PLoS One*, **6**(10), e25649.
- Schwartzman, J.A., Koch, E., Heath-Heckman, E.A., Zhou, L., Kremer, N., McFall-Ngai, M.J., et al. (2015) The chemistry of negotiation: rhythmic, glycan-driven acidification in a symbiotic conversation. *Proceedings of the National Academy of Sciences USA*, **112**(2), 566–571.
- Singh, P., Brooks, J.F. 2nd, Ray, V.A., Mandel, M.J. and Visick, K.L. (2015) CysK plays a role in biofilm formation and colonization by *Vibrio fischeri*. *Applied and Environment Microbiology*, **81**(15), 5223–5234.
- Stabb, E.V. and Ruby, E.G. (2002) RP4-based plasmids for conjugation between *Escherichia coli* and members of the *Vibrionaceae*. *Methods in Enzymology*, **358**, 413–426.
- Stacy, A., McNally, L., Darch, S.E., Brown, S.P. and Whiteley, M. (2016) The biogeography of polymicrobial infection. *Nature Reviews Microbiology*, **14**(2), 93–105.
- Stoudemire, J.L., Essock-Burns, T., Weathers, E.N., Solaimanpour, S., Mrazek, J. and Stabb, E.V. (2018) An iterative synthetic approach to engineer a high-performing PhoB-specific reporter. *Applied and Environment Microbiology*, **84**:e00603-18.
- Studer, S.V., Schwartzman, J.A., Ho, J.S., Geske, G.D., Blackwell, H.E. and Ruby, E.G. (2014) Non-native acylated homoserine lactones reveal that LuxIR quorum sensing promotes symbiont stability. *Environmental Microbiology*, **16**(8), 2623–2634.
- Sun, Y., Verma, S.C., Bogale, H. and Miyashiro, T. (2015) NagC represses *N*-acetyl-glucosamine utilization genes in *Vibrio fischeri* within the light organ of *Euprymna scolopes*. *Frontiers in Microbiology*, **6**, 741.
- Sun, Y., LaSota, E.D., Cecere, A.G., LaPenna, K.B., Larios-Valencia, J., Wollenberg, M.S., et al. (2016) Intraspecific competition impacts *Vibrio fischeri* strain diversity during initial colonization of the squid light organ. *Applied and Environment Microbiology*, **82**(10), 3082–3091.
- Verma, S.C. and Miyashiro, T. (2013) Quorum sensing in the squid-*Vibrio* symbiosis. *International Journal of Molecular Sciences*, **14**(8), 16386–16401.
- Verma, S.C. and Miyashiro, T. (2016) Niche-specific impact of a symbiotic function on the persistence of microbial symbionts within a natural host. *Applied and Environment Microbiology*, **82**(19), 5990–5996.
- Visick, K.L., Foster, J., Doino, J., McFall-Ngai, M. and Ruby, E.G. (2000) *Vibrio fischeri lux* genes play an important role in colonization and development of the host light organ. *Journal of Bacteriology*, **182**(16), 4578–4586.
- Wollenberg, M.S. and Ruby, E.G. (2009) Population structure of *Vibrio fischeri* within the light organs of *Euprymna scolopes* squid from Two Oahu (Hawaii) populations. *Applied and Environment Microbiology*, **75**(1), 193–202.

Supporting information

Additional supporting information may be found online in the Supporting Information section at the end of the article.